Pyro-electrolytic water splitting for hydrogen generation

Yan Zhang [a, b], Santosh Kumar [c], Frank Marken [d], Marcin Krasny [a], Eleanor Roake [a], Salvador Eslava [c], Steve Dunn [e], Enrico Da Como [f], Chris R. Bowen [a]

[a] *Department of Mechanical Engineering, University of Bath, Bath, BA2 7AY, UK*

[b] *State Key Laboratory of Powder Metallurgy, Central South University, Changsha, China*

[c] *Department of Chemical Engineering, University of Bath, Bath, BA2 7AY, UK*

[d] *Department of Chemistry, University of Bath, Bath, BA2 7AY, UK*

[e] *Chemical Engineering, School of Engineering, London South Bank University, 103 Borough Road, London, SE1 0AA, UK*

[f] *Department of Physics, University of Bath, Bath, BA2 7AY, UK*

Abstract: Water splitting by thermal cycling of a pyroelectric element acting as an external charge source offers an alternative method to produce hydrogen from low grade waste heat or natural temperature changes. In contrast to conventional energy harvesting, where the optimised load resistance is used to maximise the combination of current and voltage, for water splitting applications there is a need to optimise the system to achieve a sufficiently high potential difference for water electrolysis, whilst maintaining a high current output. For the thermal harvesting system examined here, a high impedance 0.5 M KOH electrolyte with working electrodes connected to a rectified pyroelectric harvester produced the highest voltage of 2.34 V, which was sufficient for H_2 generation. In addition to electrolyte concentration, the frequency of the temperature oscillations was examined and reducing the heating-cooling frequency helped to produce a larger change in temperature to generate more pyroelectric charge and a higher potential difference for pyro-water splitting. Finally, in the absence of sacrificial reagents, cyclic production of H_2 (0.654 μmol/h) was demonstrated with the optimised processing parameters of electrolyte and thermal cycling frequency via the external pyroelectric water splitting route.

Keywords: water splitting, pyroelectric, external power source, H_2 generation

1. Introduction

Carbon dioxide emission from traditional carbon based sources of energy such as coal, oil and natural gas has been a significant contributor to global warming and climate change. Therefore, interest in alternative and renewable fuels for energy sources has increased rapidly worldwide. In this regard, hydrogen fuel can contribute significantly to the future energy mix, since it has the attractive features of being a clean and sustainable energy source with a high energy density and no greenhouse gas emission when burned in the oxygen. However, over 90% of hydrogen is currently produced from fossil fuels and biomass, which is high cost and the processing route produces further greenhouse gases as a by-product [1]. To address these problems, hydrogen generation by water electrolysis (or water splitting) using electricity or solar energy has attracted significant attention [2-5].

A common approach to generate hydrogen by water splitting is to employ a wide band semiconductor [2, 4, 6] that can absorb sunlight and generate photo-excited carriers to electro-chemically reduce and oxidize water. However, the range of potential materials is limited [7] and material lifetime and performance remains a challenge. As an alternative approach, exploiting the pyroelectric effect to produce hydrogen from time-temperature variations has emerged recently as potential approach to generate hydrogen from transient low grade waste heat (< 100 ˚C) or natural temperature changes [8-13], which can also be converted by the thermoelectric effect for static conditions [14]. Sunlight and wind have also been considered to generate temperature oscillations [15]. A pyroelectric material is highly polarised, and when the temperature of the material is increased the polarisation level falls, which releases electrical charge on its surface [16]. On cooling the polarization increases, reversing the electric current flow as charge is attracted to the more polarized surface.

If we consider a water splitting application, the amount of available charge (Q) generated by a temperature change (ΔT) of a pyroelectric is given by;

$$Q = p \cdot A \cdot \Delta T \qquad (1)$$

where p is the pyroelectric coefficient (C m^{-2} K^{-1}) and A is the surface area (m^2) of the material. While the amount of charge generated is related to the area of the pyroelectric, the potential (V) developed across a pyroelectric is dependent on its thickness (h), and is given by;

$$V = \frac{p \cdot h \cdot \Delta T}{\varepsilon_0 \varepsilon_{33}} \qquad (2)$$

where ε_{33} is the relative permittivity of the material and ε_0 is the permittivity of free space. Since Q is proportional to the surface area (Eqn. 1) and V is proportional to thickness (Eqn. 2), there is potential to design the optimum geometry of the pyroelectric elements for electrolysis; where

the thickness can be used to ensure a sufficient potential is produced to initiate water splitting and the area should be maximized for harvesting the greatest amount of available surface charge.

An overview of coupling energy harvesting devices to electro-chemical systems has been recently provided by Zhang et al [17]. To date, pyroelectric energy harvesting using thermal fluctuations or/and transient waste heat has been utilized for water related electro-chemical reactions, in terms of water treatment [9, 10, 18-28], and for water splitting applications only a small amount of work has been undertaken [8, 11, 12, 29, 30]. The first experimental evidence of pyroelectric water splitting was reported by the comparison of bulk lead zirconate titanate (PZT) and polymer ferroelectrics as an external charge source [30]. The materials were thermally cycled at a fixed frequency and electrolyte, and direct measurements of hydrogen and oxygen generation were not reported. Belitz *et al.* recently explored pyroelectric water splitting by placing a crushed and polarised $BaTiO_3$ single crystal powder into direct contact with water, and thermal cycling the mixture from 40 to 70°C [12]. The advantage of this Internally Positioned Pyroelectric (IPP) approach is that using finely dispersed pyroelectric particulates suspended in the electrolyte enables the area of the pyroelectric to be increased, and therefore the available charge for hydrogen production; see Eqn. 1. In terms of modeling a pyroelectric induced water splitting process, Kakekhani et al. developed a density functional theory (DFT) model of a ferroelectric lead titanate ($PbTiO_3$) material and examined the impact of thermal cycling of the ferroelectric as it is heated and cooled above below it Curie temperature (T_c) in the presence of water molecules [8]. The work showed that cycling between the low temperature ferroelectric state and high temperature paraelectric state provides scope to harvest thermal fluctuations and produce hydrogen. Xu et al. recently presented experimental data of $Ba_{0.7}Sr_{0.3}TiO_3$ powders suspended in an electrolyte, achieving a hydrogen production of 46.89 mol per gram of the powder after 36 thermal cycles above and below its Curie temperature [11]. Pyroelectric two-dimensional black phosphorene has also been reported as a charge source under thermal cycling for both hydrogen generation and dye decomposition [10]. The charge generated by pyroelectrics subjected to hot-cold cycles has also been used for dye decomposition using $BaTiO_3$ particles [9] and $NaNbO_3$ nanofibers [20].

However, potential challenges for pyroelectric water splitting using a material in powder form that is suspended in the electrolyte for practical large-scale applications is the need to collect the dispersed powder and separate the hydrogen and oxygen gas when formed, leading to low efficiency of the water splitting process. In addition, due to the hydrolysis of the ceramic powder, pH changes during the process can affect kinetic behavior during water splitting. In

contrast, the use of an externally positioned pyro-electrolysis (EPP) is accompanied by the flow of a rectified electric current through an external circuit in the water splitting system. Compared to water splitting using suspensions in an electrolyte, the EPP system has the advantage that there is no need for gas separation because the generation of H_2 and O_2 is spatially separated from different electrode sides, which is beneficial for high hydrogen production and simplifying hydrogen and oxygen separation. Moreover, the external pyro-charge provider can be easily collected compared with the internal powder form.

Preliminary work has been undertaken on the potential of pyroelectric materials and geometries for externally pyroelectric water electrolysis, which demonstrated that thin layers of lead zirconate titanate (PZT) are promising for H_2 generation [30]. This work utilizes PZT as an external charge source that undergoes hot-cold thermal cycles for pyro-electric water splitting; the work has a focus on the optimization of system parameters, such as electrolyte impedance and heating-cooling cyclic frequency and its effect on the current, voltage and generated power were systematically examined. In addition, the resulting H_2 production is detected, quantified and corresponding efficiency also evaluated. Finally, the resulting H_2 generation from the optimized conditions were explored and measured. This is the first time to understand and systematically examine the processing parameters (frequency and electrolyte impedance) for externally H_2 generation based on the pyroelectric effect and to measure and quantify the amount of hydrogen and oxygen generated.

2. Experimental section

2.1 Material and heat source

For the pyro-electrolysis water splitting, a commercial dense and thin PZT sheet (PSI-5H4E, Piezo system, inc. USA) with a thickness of 127 μm and surface area of 49 cm^2 was utilised as the external pyroelectric charge source that is subjected to thermal cycles outside of the electrolyte [30]. The surface of both sides of the PZT sheet were covered by the vacuum sputtered nickel electrode. For the electrolyte, KOH solutions with a variety of concentrations of 0.5, 1, 2, 3 M were employed for H_2 generation to examine the influence of electrolyte impedance on output voltage and current (4 M KOH was also prepared for the impedance analysis). During the pyroelectric initiated water splitting reaction, the PZT sheet was heated by irradiating with an infrared heat lamp whose maximum light intensity of ~370 mW/cm^2, which was placed at a fixed distance of 13 cm from the PZT surface. Varying heating cycles at frequencies of 0.05, 0.1, 0.2 and 0.3 Hz were used to examine the impact of frequency on

voltage and current. At the same time a thermoelectric Peltier cooling system was also supplied to cool down the PZT sheet in a periodic fashion. This combination of heating and cooling provided a continuous and controlled periodic heating and cooling cycles to achieve a pyroelectric response for the PZT sheet, while in a harvesting application the material may be subjected to a range of waste heat or natural thermal transients. A Type K thermocouple was used to monitor the temperature of the surface of the pyroelectric element. As another alternative way to provide the thermal fluctuation, a fan was coupled to the pyroelectric energy harvesting system, where the heat from the sunlight can be periodic applied to provide the thermal fluctuation on the pyroelectric element [15].

2.2 Electrical characterisation and H_2 detection

The polarisation-field hysteresis loop of the PZT sheet was measured by a Radiant RT66B-HVi ferroelectric test system to confirm its ferroelectric response. The impedance of the KOH electrolytes from 1 Hz to 1 MHz was measured by an impedance analyzer (Solartron 1260, Hampshire, UK) at room temperature. The current levels produced by different concentrations of the electrolytes under the applied DC voltages from -4 V to 4 V were performed with a commercial potentiostat (Compact Stat, Ivium Technologies) to characterise the cell used for the water splitting which consisted of counter electrode, working electrode, the I/E converter, the control amplifier, and the signal.

During thermal cycling of the pyroelectric element for water splitting an ac-dc converter composed of a rectifier bridge circuit was used to provide a unipolar output so that hydrogen and oxygen were produced at different electrodes. An electrometer (Model 6517B, Keithley Instruments, Cleveland, OH) was used to measure the voltage and current in the circuit accurately. Before applying the thermal fluctuation, ultra-pure N_2 gas was introduced to purge the electrolysis cell by bubbling through the electrolyte for 0.5 h to remove residual air. The produced hydrogen and oxygen gases were evolved and analysed by the gas chromatography (GC) system (GC, Vairan3800), using ultra-pure Ar (99.9995 vol.%) as carrier gas and a thermal conductivity detector (TCD).

3. Results and discussion

3.1 Basic mechanism involved in pyroelectric water splitting

Fig. 1(A) shows a schematic of the setup utilised to carry out the water splitting reaction with the pyroelectric material externally positioned. The mechanism consists of three main steps where, firstly, charges with negative and positive signs are separately generated on the surface of the pyroelectric element (inset of Fig. 1(A)) that is subjected to thermal fluctuations. The AC electrical output from the pyroelectric generator is then rectified through an external circuit to act as the DC input to the electrolysis cell where electrons move to the cathode in the cell. The H^+ in the water is then reduced to produce H_2 on the cathode surface, where O_2 is simultaneously produced at the anode. The change of the polarisation (*dP/dt*) of the ferroelectric during thermal cycling with time is the driving force for the pyroelectric charge generation during hot-cold fluctuations. Fig. 1 (B) shows the PZT sheet used in this experiment whose remnant polarisation, saturation polarisation and coercive field are ~20 $\mu C/cm^2$, 28 $\mu C/cm^2$ and 26 kV/cm observed from the hysteresis loop shown in Fig. 1(C). This high polarisation is the primary reason for the excellent piezo-, pyro- and ferro-electric properties of PZT compared with ferroelectric polymers and lead-free materials [31]. This is a widely-used piezo-material, which is a Type 5H (Navy Type VI) piezoelectric ceramic, with typical pyroelectric coefficients of ~450 $\mu C\ m^{-2}\ K^{-1}$ [32]. In this work, under cyclic hot-cold fluctuations at a frequency of 0.1 Hz, the change of the temperature ΔT on the surface of the PZT sheet was ~3 °C, with a corresponding rate of change of temperature with time, dT/dt ~ 0.16 °C/s. The generated bipolar voltage and current outputs were shown in Fig. S1(C) and S1(E). After rectification, the resultant unipolar peak-peak voltage and current were 8.36 V and 11.25 μA, while the peak voltage and current were 9.58 V and 13.21 μA, respectively, as shown in Fig. S1(D) and S1(F). Moreover, a range of PZT sheets with a constant thickness of 127 μm but different surface areas (*A*) were utilised to explore the current in the electrolyte and the voltage between cathode and anode produced from PZT sheet, shown in Fig. S2. With the increase of the surface area, the voltage was unchanged at ~2.3 V, since the thickness is unchanged (see Eqn. 2). However, the peak current increased almost linearly from 1.75 µA to 14.21 µA on increasing the surface area from 12.25 cm^2 to 98 cm^2, due to the linear relationship between the pyroelectric current (*I*) and surface area (*A*) of $I=P\cdot A\cdot dT/dt$ [33] at a specific rate of the temperature change *dT/dt*.

When an externally positioned pyro-electrolysis process is utilized for H_2 generation, the whole system can be considered as an analogue of a series RC circuit where the pyroelectric element can be regarded as the power source and the capacitance (*C*), while the electrolyte

acts as the external resistance load (*R*). The voltage created by the pyroelectric generator in response to a temperature change can be divided into two parts, where one part is used for triggering the electrolysis process for H_2 and the other is acting as a normal resistor in the circuit. The critical voltage for the oxidation potential of H_2O to H_2 is ~1.23 V, where an overpotential is also required to overcome the kinetic barrier for the hydrogen evolution reaction [34]. When subjected to the thermal excitation, the speed of the thermal cycling (frequency) will influence the total temperature change (ΔT) of the pyroelectric material that leads to a change of polarisation, since $dP = p \cdot \Delta T$. In this case, the higher the change in polarisation, the larger the driving force to generate a potential difference (see equation 2). Moreover, a larger ΔT is advantageous to achieve more charge based on the equation (1). Therefore, in this EPP system for H_2 generation, there is a balance between the high voltage necessary to split the water molecule (a high ΔT) and a high current (high dT/dt and more total charge) for hydrogen ion (H^+) reduction. This can be adjusted by changing either the concentration of the electrolyte or the frequency of the hot-cold fluctuation, which will be discussed later in detail.

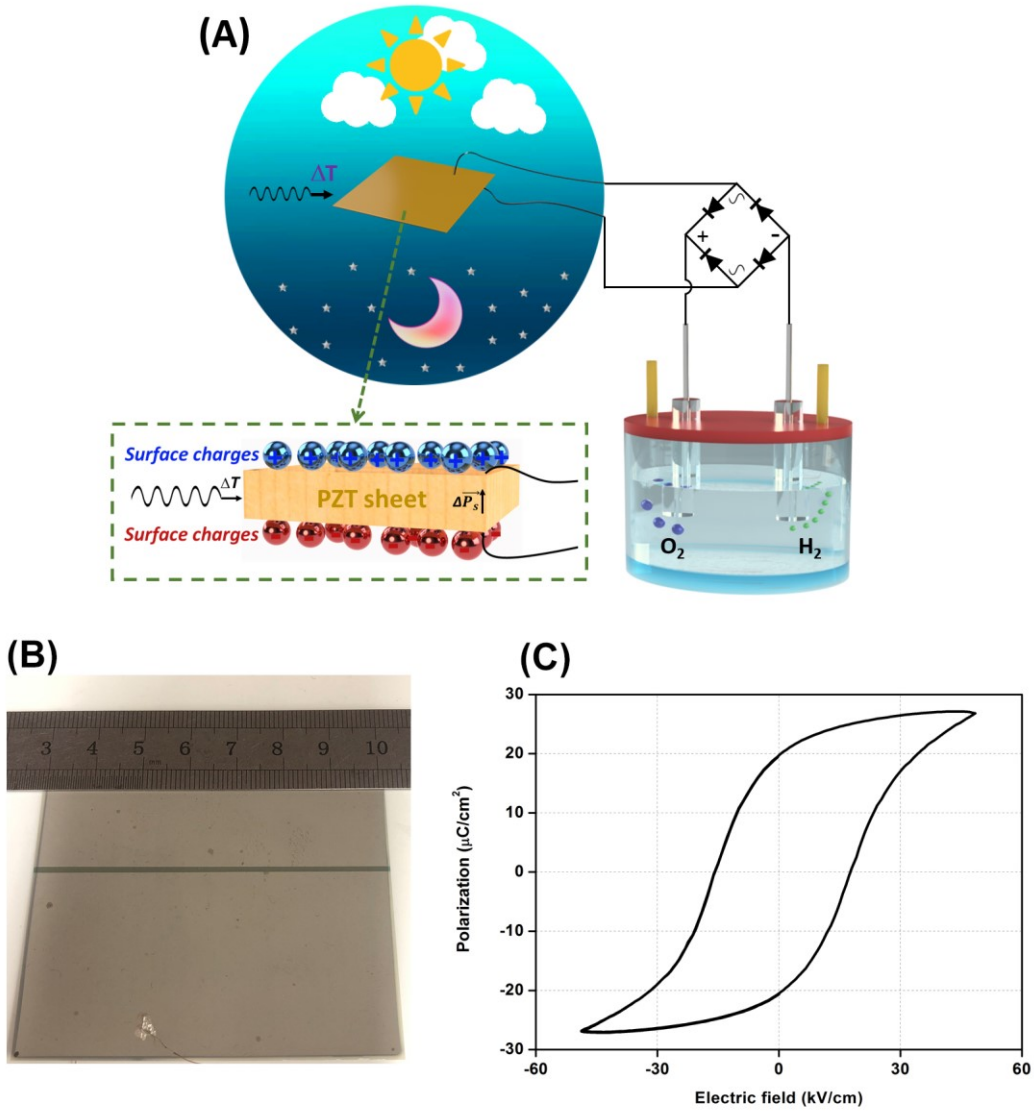

Figure 1 (A) Schematic of pyroelectric as an external source for water splitting, (B) photo of the PZT film, (C) polarisation-electric field loop of PZT sheet and schematic of the surface pyroelectric charges (inset).

Figure 2 (A) shows the current-voltage (I-V) curves of different concentrations of KOH electrolytes, without a pyroelectric element or rectifier attached to the cell. A plateau exists at all the ranges of KOH concentrations with a potential difference of approximately -1.2 V to 1.2 V where there is no current flow between the electrodes. When the absolute value of voltage was higher than 1.2 V, the current increased where small potential changes lead to large changes in current and bubbles are observed at each electrode. A rapid increase is especially observed when the potential was higher than 2.2 V, as shown in Fig. 2 (B), demonstrating the electrolysis of water. Clearly, any pyroelectric generator must also generate such potentials (> 2.0 V) to achieve water splitting. Figure 2 (C) shows the frequency dependence of electrical

impedance of different concentrations of KOH electrolytes (0.5, 1, 2, 3 M). The impedance of the KOH solutions for all concentrations decreased with an increase of frequency, due to concentration polarisation at low frequencies. As expected, the electrolyte impedance decreased with increasing KOH concentration at a particular frequency; since the thermal cycles to be employed later in this paper are typically ~ 0.1 Hz the gradual reduction in impedance with increasing KOH concentration is shown in Fig. 2 (D). When the pyroelectric generator is coupled to the electrochemical cell and subjected to thermal cycling, the resulting peak voltage and current obtained during periodic heating are summarised in Fig. 2 (E). Examples of typical generated voltage and current profiles with time obtained for the different concentrations of KOH are shown in Fig. 3. Figure 3(B), (D), (F), (H) show that when there is a decrease in KOH concentration, the peak voltage increases since it is more difficult for the pyroelectric element to discharge due to the high impedance of the electrolyte. This also resulted in the current decreasing with decreasing KOH concentration; see Figure 3(A), (C), (E), (G). In theory, when the energetic requirements are met, namely the critical potential of ~1.23 V, the water splitting reaction will occur. However, the practical potential will be higher due to the existence of overpotential and/or other system losses [35]. Based on the observation from the I-V curves presented in Fig. 2(A) and (B), a voltage higher than 2.2 V was beneficial to achieve water splitting, and a voltage of 2.34 V was generated by the pyroelectric element coupled to the higher impedance 0.5 M KOH solution.

In conventional energy harvesting systems coupled to an electrical load, such as a simple resistor, it is common to calculate the peak power and match the electrical load (R_L) to the capacitive impedance of the energy harvester; for example by achieving the condition $2\pi fC_p=1/R_L$ where C_p is the capacitance of the pyroelectric element and f is the frequency. The peak power (P_{out}) of the pyroelectric element was calculated with the standard power relationships ($P_{out} = VI$) of voltage and current, shown in Fig. 2(E), where the resistive load is the electrolyte resistance. It can be seen in Fig. 2(F) that as the KOH concentration increased from 0.5 M to 3 M, the peak power and peak power density increased from 16.9 μW (27.2 μW/cm^3) to 19.2 μW (30.8 μW/cm^3) followed by a decrease to 16.9 μW (27.2 μW/cm^3) at the highest concentration 4 M KOH; where a heating-cooling frequency of 0.1 Hz was utilised. In an R-C circuit, by matching the load and generator impedances at $2\pi fC_p=1/R_L$ the power generated reaches a maximum value since this provide a good combination of voltage and current. Based on a frequency of 0.1Hz and a capacitance of 650 nF for the pyroelectric element the optimum resistance was calculated to be approximately 2.5 MΩ, which is comparable to that of the 3 M KOH electrolyte (see Figure 2(D)). For a harvester coupled to an electrochemical system, optimisation of the system is different to a simple electrical load.

While the peak power was obtained at 3 M KOH (Fig. 2(F)) with a rectified peak voltage of 1.58 V (Fig. 2(E)) and high current of ~12 µA (Fig. 2(B)), the need for a sufficiently high voltage plays a more important role for water splitting (Fig 2(A)), therefore the 0.5 M KOH with the ability to generate the highest voltage (2.34 V) and micro-level current (~7 µA) from the PZT during thermal cycling was chosen as the electrolyte for periodic heating-cooling frequency exploration. This also correlated with visual observation of hydrogen bubbles generated within the cell during thermal cycling.

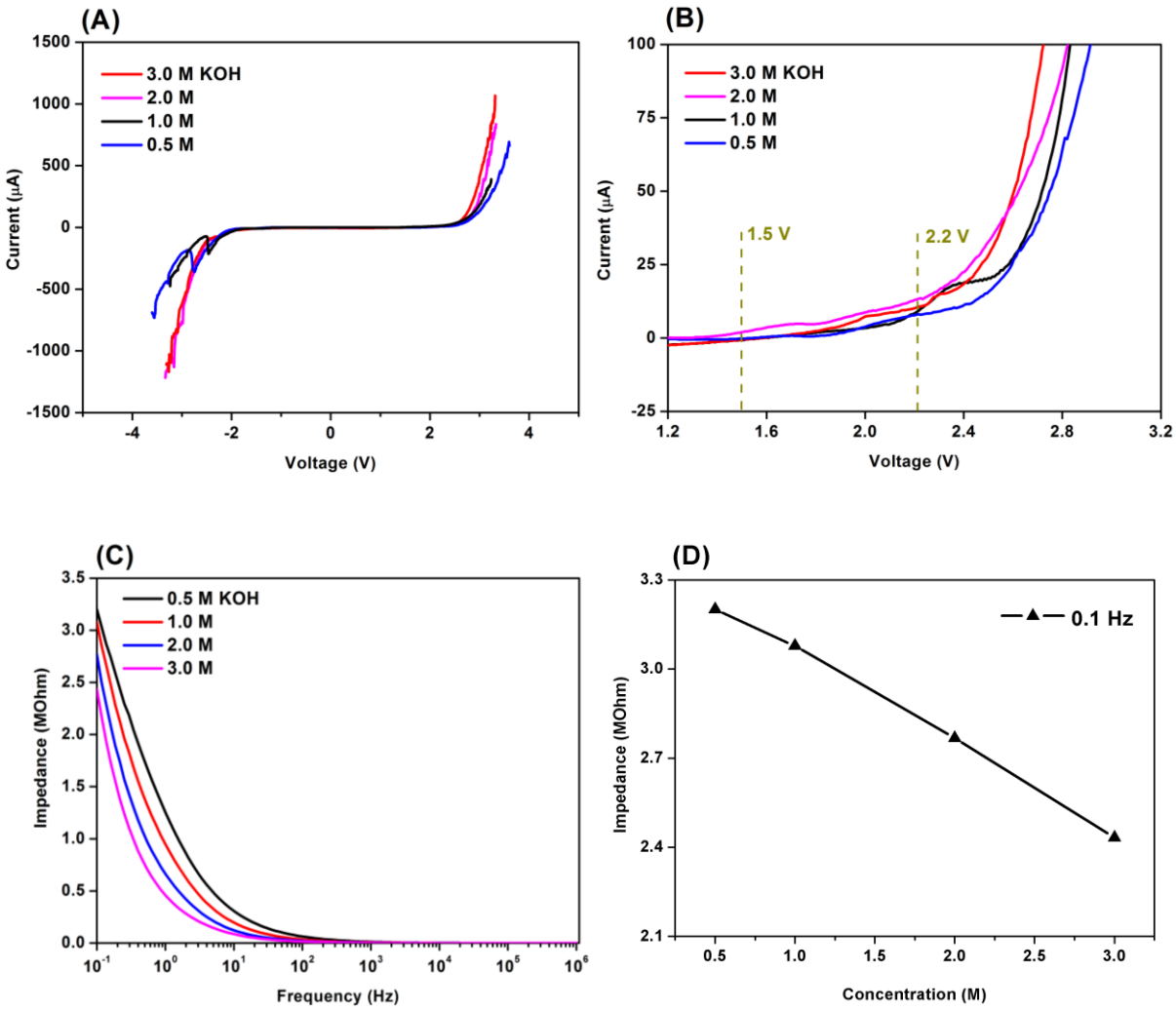

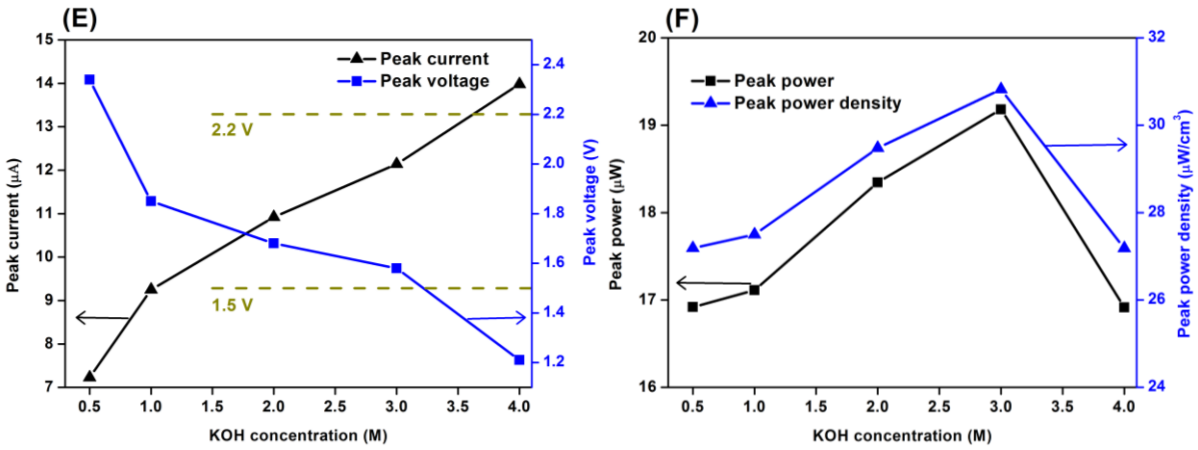

Figure 2 (A) Current-voltage characteristics with different concentrations of KOH, (B) a zoom-in current-voltage curve of (A), impedance of the KOH solutions (C) with the frequency sweeping from 0.1 Hz to1 MHz and (D) fixed at 0.1 Hz, (E) peak voltage and current measured from different concentrations of KOH produced by the pyroelectric PZT sheet, (F) the corresponding peak power and peak power density calculated based on (E).

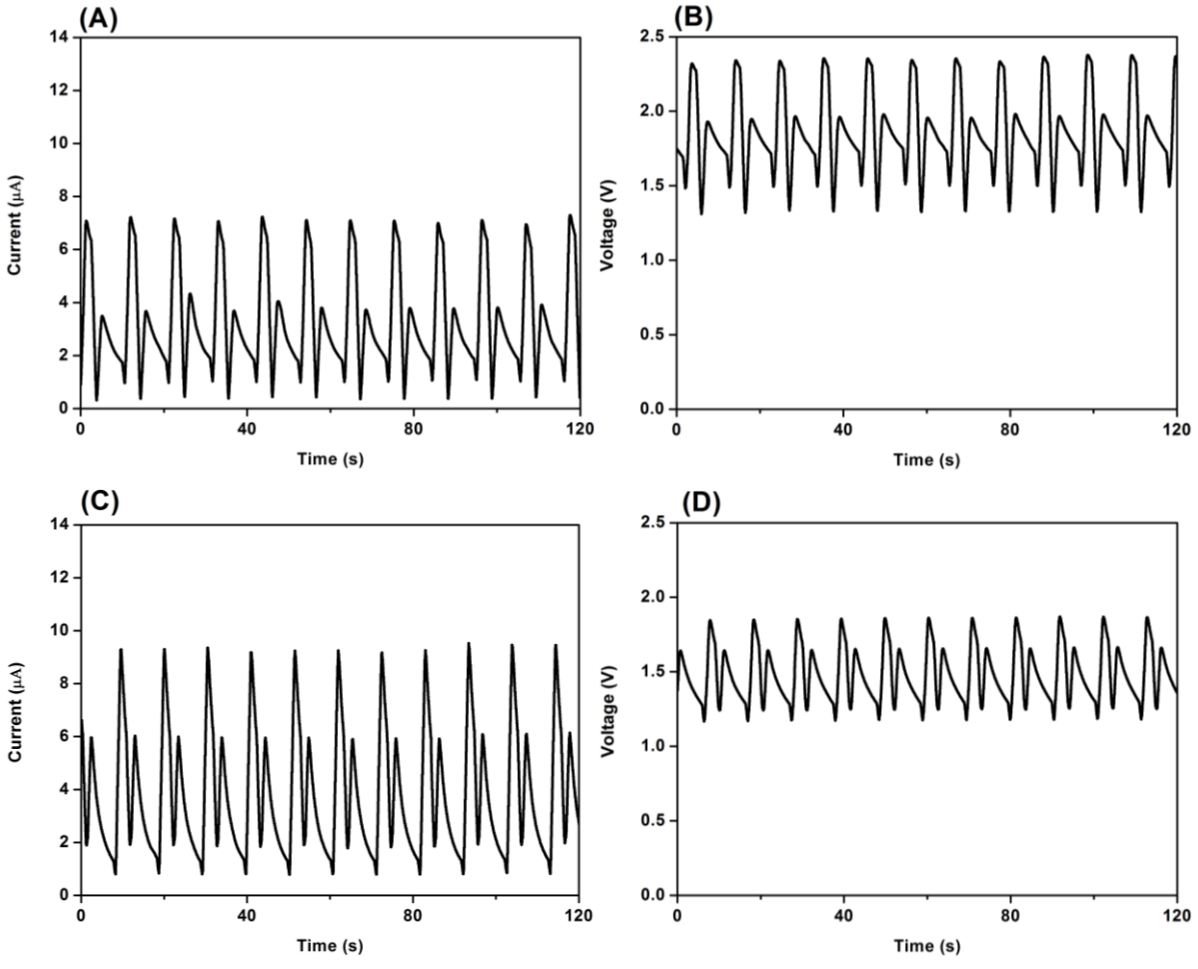

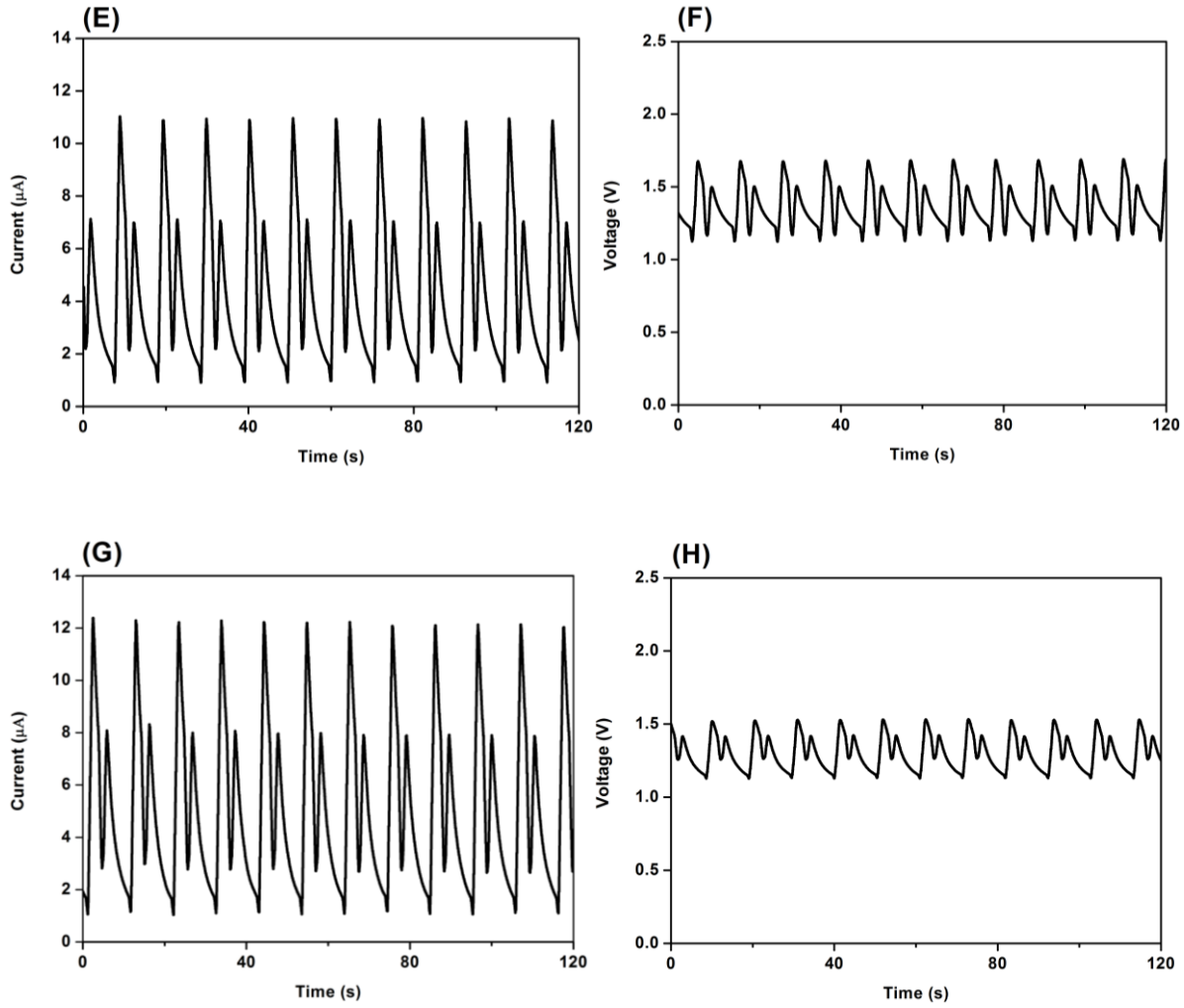

Figure 3 Effect of different concentrations on the rectified current (A) 0.5 M, (C) 1.0 M, (E) 2.0 M, (G) 3.0 M, and voltage (B) 0.5 M, (D) 1.0 M, (F) 2.0 M, (H) 3.0 M of the KOH electrolyte, with periodic heating and cooling at a frequency of 0.1 Hz.

Figure 4 shows the change of the temperature (ΔT) on the PZT surface and the resultant peak voltage and current in the 0.5 M KOH electrolyte with periodic heating-cooling frequencies ranging from 0.05 to 0.3 Hz. As can be seen from Fig. 4(A)-(D), the change of temperature decreased with an increase in frequency. It is noted that ΔT obtained from 0.1 Hz (2.9 °C) has a small drop compared to that of 0.05 Hz (3 °C) while large decreases were found in those of 0.2 Hz (2.1 °C) and 0.3 Hz (1.3 °C), shown in Fig. 4(E). At a low frequency, the pyroelectric element was exposed to the heat source for longer period of time, allowing greater heat transfer through its thickness, which leads to a more homogeneous temperature distribution. From the Eqn. (1) and (2), the larger the temperature change (ΔT) of the pyroelectric, the greater the generated charge (Q) and potential difference (V) produced, leading to the more electrons to reduce the H^+ in the electrolyte and higher potential as the driving force to split

water. This was in agreement with the obtained peak voltage and current in the 0.5 M KOH electrolyte, shown in Fig. 4(F). A small decrease of the peak voltage (2.35 V/ 2.34 V) and current (7.27 μA/ 7.23 μA) was found on increasing the frequency from 0.05 Hz to 0.1 Hz, while a sharp drop was observed for the 0.5 M KOH electrolyte on increasing the frequency from 0.2 Hz to 0.3 Hz, e.g. a fall to 1.11 V and 2.21 μA when an oscillation frequency of 0.3 Hz applied. The voltage/current generation profiles obtained via a range of periodic heating-cooling frequencies are shown in Fig. S3 and the corresponding power and power density are shown in Fig. S4. Understanding the frequency dependence of change in polarisation would be of interest for further studies for this application, for example by laser intensity modulation method (LIMM) which has been used to characterise pyroelectric materials [36]. In this work we have selected a relatively low frequency of 0.1Hz for the final detection of H_2 an quantification since it is the highest frequency that is able to achieve a change in temperature which is sufficient to produce a voltage >2 V for water splitting. There is also a small difference of the generated voltage and current in the electrolyte between the frequencies of 0.05 and 0.1 Hz, see Fig 4(F).

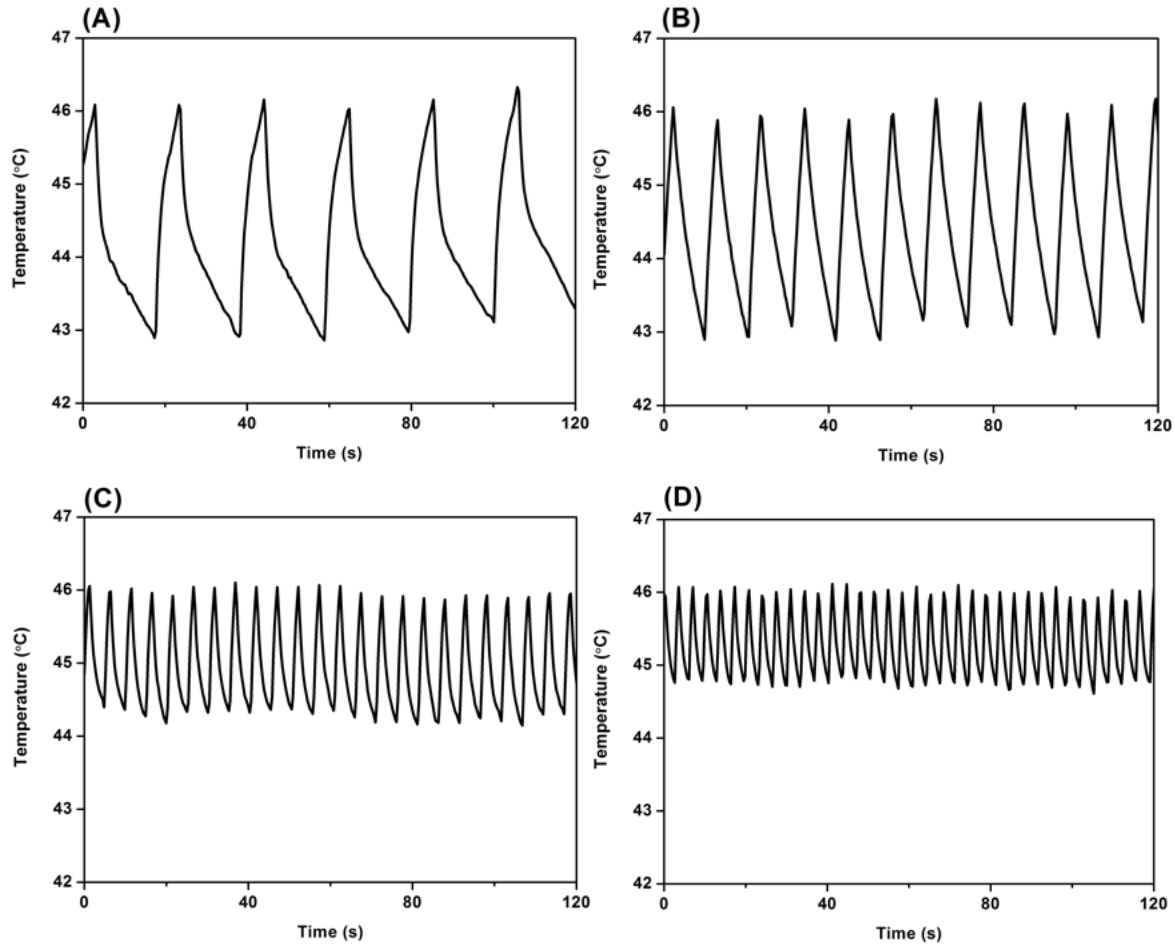

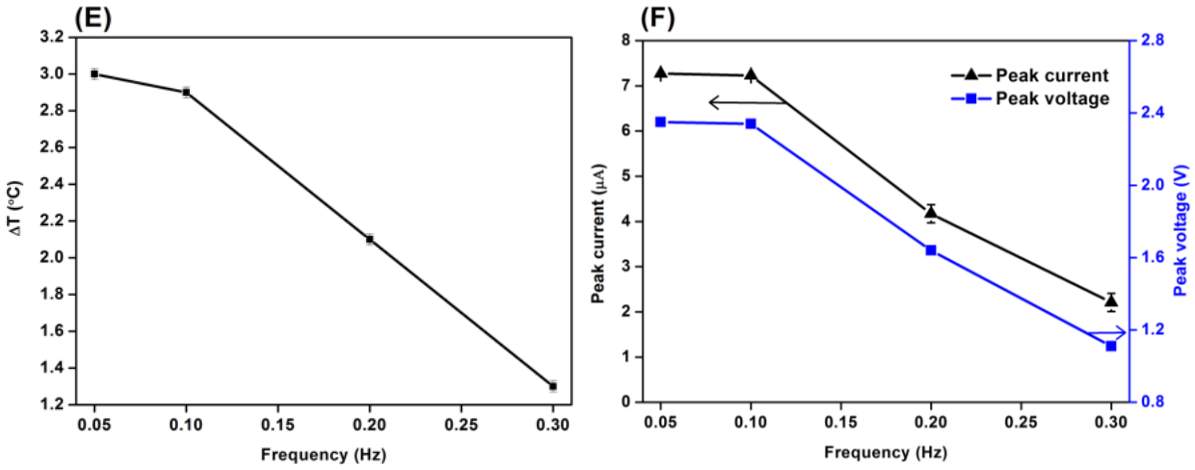

Figure 4 Change of temperature (ΔT) with different heating-cooling frequencies in terms of (A) 0.05 Hz, (B) 0.1 Hz, (C) 0.2 Hz, and (D) 0.3 Hz, and (E) the relationship between ΔT and frequency, (F) produced peak current and voltage.

Figure 5 shows the production of oxygen and hydrogen from the pyroelectric induced electro-chemical reaction using a KOH concentration of 0.5 M, with periodic heating and cooling at a frequency of 0.1 Hz. In terms of the charge Q, the higher the temperature the more it will be produced (see Eqn.1). However the total charge per time is also related to the frequency of the temperature fluctuations and the output voltage. Therefore where using thermal cycling via the lamp, there is a balance between the frequency of thermal cycles, the achievable temperature change and achieving a sufficient potential difference for water splitting (2.34 V). For example, see Figure 4 where increasing the frequency leads to a reduction in the achievable temperature. As a result, in this work we have selected a relatively low frequency of 0.1 Hz since it is the highest frequency that is able to achieve a change in temperature which is sufficient to produce a voltage >2 V for water splitting. Lower frequencies e.g. 0.05 Hz (see Figure 4) could achieve only slightly high temperature changes (and therefore charge per cycle) but at this low frequencies the total charge over time is lower. As an example of real-time water splitting process during thermal cycling is shown in the video (Video. S1). As can be seen from Fig. 5(A), the degree of H_2 evolution increased from 0.38 μmol to 3.93 μmol with increasing build-up time (1-6 h). The H_2 evolution production increased slowly from 1 to 3 hours with the slope of 0.38 μmol/h, with an increase of the H_2 production with the slope of 1.06 μmol/h was achieved at longer times from 4 to 6 hours. The change in production rate is thought to be due a surface conditioning phenomenon where the physical roughness, adsorbed impurities and surface oxides on the surface of the electrode are changing with time, which is commonly observed for plantinum elctrodes [37]. The production of continuous bubbles of hydrogen and oxygen during each thermal cycle from the electrodes and the corresponding amount of H_2 and O_2 and

evolution rate after 6 h is presented in Fig. 5(B); the ratio of H_2 and O_2 is approximately 2:1, as would be expected for the reaction $2H_2O \rightarrow 2H_2 + O_2$. In this system, the pyroelectric induce water-splitting produced both hydrogen and oxygen simultaneously on separate electrodes, without the consumption of the sacrificial reagents or hole scavengers [10, 11]. According to Faraday's law, $m = \frac{QM}{Fz}$, where *m* is the mass of the substance altered at an electrode which is H_2 in this work, *Q* is the total electric charge passed through the substance, *F* = 96.485 C mol^{-1} is the Faraday constant, *M* is the molar mass of the substance, and *z* is the valance number of ions of the substance, the theoretical mole (m/M) of generated H_2 can be predicted based on the charge generated from the pyroelectric PZT sheet under thermal fluctuation, and the comparison with the experimental measured date is shown in Fig. 5(C). The Faradic efficiency of pyro-electrolytic water splitting was calculated as ~ 10%, which was enhanced to ~15% at six hours due to surface conditioning, shown in Fig. 5(A). Table 1 summarizes the main parameters and final H_2 production between the internal (suspended pyroelectric particles in the electrolyte) and the external pyroelectric water splitting of this work. In this work, thermal fluctuations were conducted well below the Curie temperature of 350 °C to avoid the loss of remnant polarisation and to generate a continuous voltage and current, e.g. as in Fig. 3. Despite a bulk material being used, with a total PZT surface area much smaller than nano-powders [38], and a relatively small change of temperature (ΔT ~3 °C; see Table 1), pyroelectric induced water splitting using an externally source had comparable [10] or higher [11] H_2 generation performance than using the internal positioned route. Since the charge *Q* and potential *V* for pyro-water splitting are directly proportional to the area and thickness (Eqn. 1 and 2), future work could be focused on pyroelectric sheet with high pyroelectric response, high thermal conductivity or high heat transfer configurations, reduced permittivity and low Curie temperature for the external pyro-electrolytic water splitting.

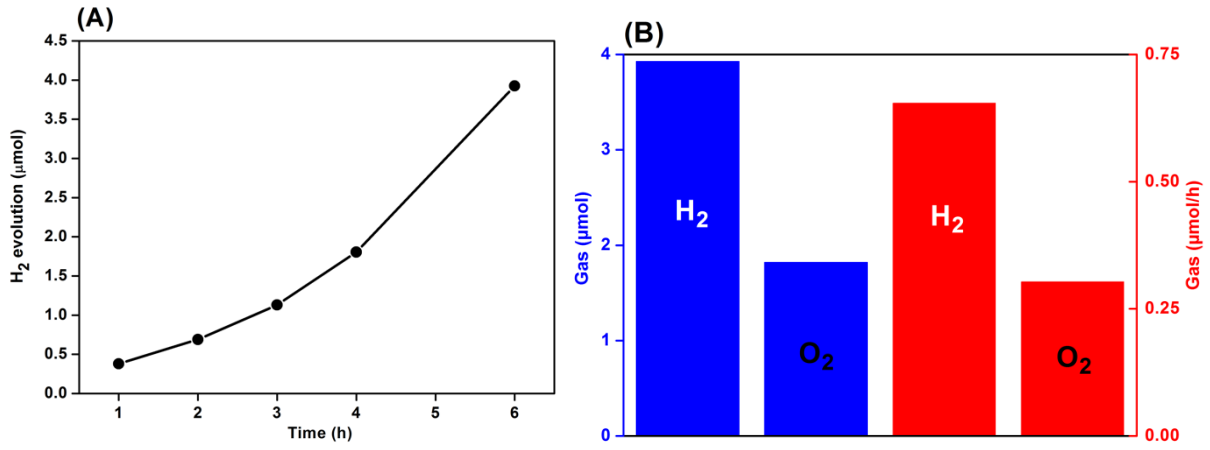

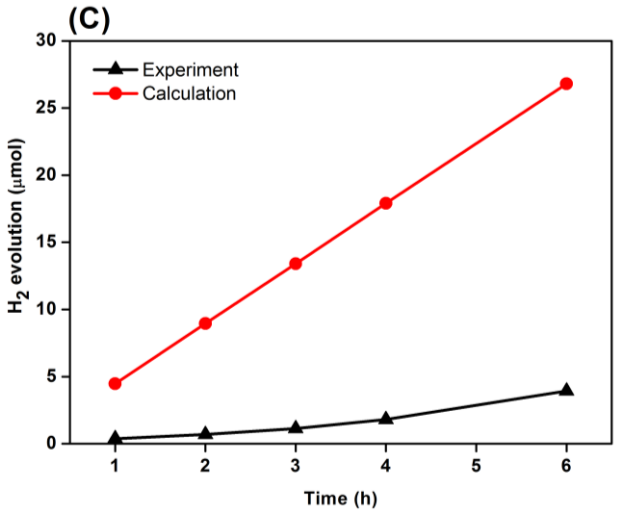

Figure 5 (A) H_2 evolution from external pyroelectric water splitting with sampling time ranging from 1 to 6 h, (B) the amount and evolution rate of H_2 and O_2 after 6 h detected from the gas chromatography and (C) comparison of the theoretical results and experimental data on the H_2 production generated with the 0.5 M of the KOH electrolyte and 0.1 Hz of the cyclic thermal fluctuation.

Table 1 Comparison of the internal and external positioned pyroelectric for water splitting.

Material	Dimension	ΔT (K)	Time	Sacrificial reagent	H_2 evolution rate	Ref
$BaTiO_3$ single crystals	<100 μm	30	Few cycles (2 min/cycle)	No	300 Vol.-ppb (part per billion)	[12]
Nano $Ba_{0.7}Sr_{0.3}TiO_3$ powders	10 mg, 200 nm, cubed shape	25	6 h	Yes	0.075 μmol/h [1]	[11]
				No	1.25 x 10^{-3} μmol/h [1]	
Nano 2D black phosphorene powders	1 mg, thickness of 0.35 nm, surface area of 9 cm^2	50	1 thermal cycle	Yes	22.5 μmol/g	[10]
PZT sheet	4.85 g, thickness of 170 μm, surface area of 49 cm^2	3	6 h	No	0.654 μmol/h	This work

[1] calculated data based on relative parameter reported in the reference.

4. Conclusions

Hydrogen production via pyro-electrolytic water splitting is a promising green process where fluctuating thermal energy, such as transient low grade waste heat and natural temperature changes can be converted into chemical energy. In this study, the effects of the electrolyte concentration and heating-cooling frequency were investigated to explore the pyroelectric H_2 generation performance. The low impedance KOH electrolyte with a concentration of 0.5 M had the maximum voltage (2.34 V) and micro-level current (~7 μA) among all the concentrations explored for a PZT element with an area of 49 cm^2; the differences in

optimisation of the electrochemical system compared to conventional electrical systems are discussed. With an increase of the heating-cooling frequency from 0.05-0.3 Hz, the change of the surface temperature of the pyroelectric decreased from 2.9 to 1.3 °C. Without the aid of the sacrificial reagents, the pyro-electrolytic water splitting with the pyroelectric externally positioned configuration was able to produce continuous H_2 gas, which was detected as 3.93 μmol in 6 h. Future work could be focused on the formation of pyroelectric nano-structures to increase the surface area of the pyroelectric element, which is proportional to the generated charge.

Acknowledgement

Dr. Y. Zhang, Mr M. Krasny and Prof. C. R. Bowen would like to acknowledge the funding from the European Research Council under the European Union's Seventh Framework Programme (FP/2007–2013)/ERC Grant Agreement No. 320963 on Novel Energy Materials, Engineering Science and Integrated Systems (NEMESIS). The Leverhulme Trust (project No. RPG-2018-290) is acknowledged by Prof. Bowen. Dr Y. Zhang also would like to acknowledge the project (Grant No. 621011812) supported by State Key Laboratory of Powder Metallurgy, Central South University, Changsha, China.

References

[1] R.M. Navarro, M.A. Peña, J.L.G. Fierro, Hydrogen Production Reactions from Carbon Feedstocks: Fossil Fuels and Biomass, Chem. Rev. 107(10) (2007) 3952-3991.

[2] M.B. Starr, X. Wang, Coupling of piezoelectric effect with electrochemical processes, Nano Energy 14 (2015) 296-311.

[3] S.A. Nahian, R.K. Cheedarala, K.K. Ahn, A study of sustainable green current generated by the fluid-based triboelectric nanogenerator (FluTENG) with a comparison of contact and sliding mode, Nano Energy 38(Supplement C) (2017) 447-456.

[4] X. Yu, X. Han, Z. Zhao, J. Zhang, W. Guo, C. Pan, A. Li, H. Liu, Z. Lin Wang, Hierarchical TiO2 nanowire/graphite fiber photoelectrocatalysis setup powered by a wind-driven nanogenerator: A highly efficient photoelectrocatalytic device entirely based on renewable energy, Nano Energy 11 (2015) 19-27.

[5] W. Tang, Y. Han, C.B. Han, C.Z. Gao, X. Cao, Z.L. Wang, Self-Powered Water Splitting Using Flowing Kinetic Energy, Adv. Mater 27(2) (2015) 272-276.

[6] Pena Pereira, Francisco, Miniaturization in Sample Preparation, De Gruyter2014.

[7] A. Fujishima, K. Honda, Electrochemical Photolysis of Water at a Semiconductor Electrode, Nature 238 (1972) 37.

[8] A. Kakekhani, S. Ismail-Beigi, Ferroelectric oxide surface chemistry: water splitting via pyroelectricity, Journal of Materials Chemistry A 4(14) (2016) 5235-5246.

[9] Y. Xia, Y. Jia, W. Qian, X. Xu, Z. Wu, Z. Han, Y. Hong, H. You, M. Ismail, G. Bai, L. Wang, Pyroelectrically Induced Pyro-Electro-Chemical Catalytic Activity of BaTiO3 Nanofibers under Room-Temperature Cold–Hot Cycle Excitations, Metals 7(4) (2017) 122.

[10] H. You, Y. Jia, Z. Wu, F. Wang, H. Huang, Y. Wang, Room-temperature pyro-catalytic hydrogen generation of 2D few-layer black phosphorene under cold-hot alternation, Nature Communications 9(1) (2018) 2889.

[11] X. Xu, L. Xiao, Y. Jia, Z. Wu, F. Wang, Y. Wang, N.O. Haugen, H. Huang, Pyro-catalytic hydrogen evolution by Ba0.7Sr0.3TiO3 nanoparticles: harvesting cold–hot alternation energy near room-temperature, Energy & Environmental Science (2018).

[12] R. Belitz, P. Meisner, M. Coeler, U. Wunderwald, J. Friedrich, J. Zosel, M. Schelter, S. Jachalke, E. Mehner, Waste Heat Energy Harvesting by use of BaTiO3 for Pyroelectric Hydrogen Generation, Energy Harvesting and Systems, 2017, p. 107.

[13] A.L. Cottrill, A.T. Liu, Y. Kunai, V.B. Koman, A. Kaplan, S.G. Mahajan, P. Liu, A.R. Toland, M.S. Strano, Ultra-high thermal effusivity materials for resonant ambient thermal energy harvesting, Nature Communications 9(1) (2018) 664.

[14] S.W. Lee, Y. Yang, H.-W. Lee, H. Ghasemi, D. Kraemer, G. Chen, Y. Cui, An electrochemical system for efficiently harvesting low-grade heat energy, Nature Communications 5 (2014) 3942.

[15] S.H. Krishnan, D. Ezhilarasi, G. Uma, M. Umapathy, Pyroelectric-Based Solar and Wind Energy Harvesting System, IEEE Transactions on Sustainable Energy 5(1) (2014) 73-81.

[16] C.R. Bowen, J. Taylor, E. LeBoulbar, D. Zabek, A. Chauhan, R. Vaish, Pyroelectric materials and devices for energy harvesting applications, Energy Environ. Sci. 7(12) (2014) 3836-3856.

[17] Y. Zhang, M. Xie, V. Adamaki, H. Khanbareh, C.R. Bowen, Control of electro-chemical processes using energy harvesting materials and devices, Chemical Society Reviews 46(24) (2017) 7757-7786.

[18] J. Wu, N. Qin, B. Yuan, E. Lin, D. Bao, Enhanced Pyroelectric Catalysis of BaTiO3 Nanowires for Utilizing Waste Heat in Pollution Treatment, ACS Applied Materials & Interfaces 10(44) (2018) 37963-37973.

[19] X. Xu, D. Chen, Z. Yi, M. Jiang, L. Wang, Z. Zhou, X. Fan, Y. Wang, D. Hui, Antimicrobial Mechanism Based on H2O2 Generation at Oxygen Vacancies in ZnO Crystals, Langmuir 29(18) (2013) 5573-5580.

[20] H. You, X. Ma, Z. Wu, L. Fei, X. Chen, J. Yang, Y. Liu, Y. Jia, H. Li, F. Wang, H. Huang, Piezoelectrically/pyroelectrically-driven vibration/cold-hot energy harvesting for mechano-/pyro- bi-catalytic dye decomposition of NaNbO3 nanofibers, Nano Energy 52 (2018) 351-359.
[21] T. Zhao, W. Jiang, D. Niu, H. Liu, B. Chen, Y. Shi, L. Yin, B. Lu, Flexible pyroelectric device for scavenging thermal energy from chemical process and as self-powered temperature monitor, Appl. Energy 195 (2017) 754-760.
[22] W. Qian, Z. Wu, Y. Jia, Y. Hong, X. Xu, H. You, Y. Zheng, Y. Xia, Thermo-electrochemical coupling for room temperature thermocatalysis in pyroelectric ZnO nanorods, Electrochem. Commun. 81 (2017) 124-127.
[23] J. Wu, W. Mao, Z. Wu, X. Xu, H. You, A.X. Xue, Y. Jia, Strong pyro-catalysis of pyroelectric BiFeO3 nanoparticles under a room-temperature cold-hot alternation, Nanoscale 8(13) (2016) 7343-7350.
[24] H. Zhang, S. Zhang, G. Yao, Z. Huang, Y. Xie, Y. Su, W. Yang, C. Zheng, Y. Lin, Simultaneously Harvesting Thermal and Mechanical Energies based on Flexible Hybrid Nanogenerator for Self-Powered Cathodic Protection, ACS Appl. Mater. Interfaces 7(51) (2015) 28142-28147.
[25] A. Benke, E. Mehner, M. Rosenkranz, E. Dmitrieva, T. Leisegang, H. Stöcker, W. Pompe, D.C. Meyer, Pyroelectrically Driven •OH Generation by Barium Titanate and Palladium Nanoparticles, J. Phys. Chem. C 119(32) (2015) 18278-18286.
[26] Y. Yang, H. Zhang, S. Lee, D. Kim, W. Hwang, Z.L. Wang, Hybrid Energy Cell for Degradation of Methyl Orange by Self-Powered Electrocatalytic Oxidation, Nano Lett. 13(2) (2013) 803-808.
[27] E. Gutmann, A. Benke, K. Gerth, H. Böttcher, E. Mehner, C. Klein, U. Krause-Buchholz, U. Bergmann, W. Pompe, D.C. Meyer, Pyroelectrocatalytic Disinfection Using the Pyroelectric Effect of Nano- and Microcrystalline LiNbO3 and LiTaO3 Particles, J. Phys. Chem. C 116(9) (2012) 5383-5393.
[28] T.F. Wiesner, Pyroelectrically-mediated reduction-oxidation reactions, Texas Tech University, 2010.
[29] A. Kakekhani, S. Ismail-Beigi, E.I. Altman, Ferroelectrics: A pathway to switchable surface chemistry and catalysis, Surface Science 650 (2016) 302-316.
[30] M. Xie, S. Dunn, E.L. Boulbar, C.R. Bowen, Pyroelectric energy harvesting for water splitting, International Journal of Hydrogen Energy 42(37) (2017) 23437-23445.
[31] J. Briscoe, S. Dunn, Piezoelectric nanogenerators – a review of nanostructured piezoelectric energy harvesters, Nano Energy 14 (2015) 15-29.
[32] R.W.W. H. H. S. Chang, and Z. Huang, Pyroelectric effect enhancement in laminate composites under short circuit condition, Journal of Applied Physics 106 (2009) 114110.
[33] C. R. Bowen, J. Taylor, E. LeBoulbar, D. Zabek, A. Chauhan, R. Vaish, Pyroelectric materials and devices for energy harvesting applications, Energy & Environmental Science 7(12) (2014) 3836-3856.

[34] T. Shinagawa, K. Takanabe, Towards Versatile and Sustainable Hydrogen Production through Electrocatalytic Water Splitting: Electrolyte Engineering, ChemSusChem 10(7) (2017) 1318-1336.
[35] L.J. Minggu, W.R. Wan Daud, M.B. Kassim, An overview of photocells and photoreactors for photoelectrochemical water splitting, International Journal of Hydrogen Energy 35(11) (2010) 5233-5244.
[36] S.B. Lang, Laser intensity modulation method (LIMM): Experimental techniques, theory and solution of the integral equation, Ferroelectrics 118(1) (1991) 343-361.
[37] A.J. Bard, Electroanalytical Chemistry: A Series of Advances, 1st Edition ed., CRC Press 1988.
[38] W. Wohlleben, J. Mielke, A. Bianchin, A. Ghanem, H. Freiberger, H. Rauscher, M. Gemeinert, V.-D. Hodoroaba, Reliable nanomaterial classification of powders using the volume-specific surface area method, Journal of Nanoparticle Research 19(2) (2017) 61.